JCSDA, Vol. 1, No. 1, 39–58
DOI: https://doi.org/10.69660/jcsda.01012403
ISSN 2959-6912

Coverage and Performance Evaluation of Multibeam Stratospheric Platforms Wireless Broadband Services

Habib Mohammed Hussien

Department of Electrical and Computer Engineering,
Artificial Intelligence and Robotics Center of Excellence,
Addis Ababa Science and Technology University,Addis Ababa, Ethiopia
habib.mohammed@aastu.edu.et

In this paper, the radiation pattern of 121 cell aperture antenna for a High-Altitude Platform (HAP) communication network via TV White Space (TVWS) spectrum is investigated. The HAP was placed 17 km above the ground with a coverage radius of 100 km and a cell radius of 10.5 km. For a co-channel cell group of 121 cells served by a payload of aperture antennas on a HAP, the effect of the antenna aperture function on co-channel interference has been explored. For each cell, the required antenna beam widths were derived from the cell's subtended angles. The proposed system coverage, re-use distance, multibeam antenna pattern, Carrier-to-interference ratio (CIR), Carrier-to-interference-plus-noise-ratio (CINR), and side lobe level values for uniform apertures were investigated. To assess the system's effectiveness, the CIR at each ground location (x, y) and the cumulative distribution function (CDF) of CINR were investigated for each co-channel cell category. The distribution of CIR levels as contour plots has been presented. The CIR values are higher at cell centers and lower at cell edges. Furthermore, the importance of minimizing the average side lobe level has been investigated. This paper demonstrated that it is possible to get a good wireless broadband performance by exploiting TVWS spectrums from HAP.

Keywords: Carrier-to-interference-ratio, carrier-to-interference-plus-noise-ratio, High altitude platform, Multi-beam, TV white space, Side lobe level.

1. Introduction

Wireless systems and their plethora of capabilities provide users with greater flexibility and ease in connecting to a variety of communication networks. Wireless solutions, with their diverse capacities, enable consumers to link to a wider range of communication networks with greater convenience and ease. These bandwidth-hungry telecommunication technologies/applications, on the other hand, placed wireless infrastructure companies under unstoppable strain to maximize the use of scarce radio resources. In this aspect, high altitude platforms (HAPs) technologies are constantly being researched, for example, in [1]-[13] as a major role in broadband wireless networking and applications, such as 3G/4G and LTE networks, WiMAX, and others. HAPs are also used for crisis monitoring and prevention as a medium of multicast coordination and emergency communication [12] and [13].

High elevation angle, line of sight communication, large coverage range, and negligible effects of wind speed and weather at an altitude of 17 - 22 km are among the several features of HAP that have attracted much interest to communication research society [1]. Telecommunication distribution that is more cost-effective and

affordable is important in locations where traffic volume is low and profit per user is predicted to be lower. HAPs may be easily and inexpensively incorporated into the networks of major mobile and internet networks to deliver a broad variety of multimedia services for locations thus preventing power from dropping in unwanted directions on the HAP and ground user. Authors in [4][6] [21][26]-[33] have evaluated the HAP communications quality with LTE, WiMAX, and White Space (TVWS). TVWS refers to the unused frequencies or gaps in the VHF and UHF spectrum, between 470 and 790 MHz to be precise. This unused frequency can be used to provide wireless internet services.

TVWS offers better mobility resilience, a longer transmission range, more penetration capabilities, and less path loss than GHz bands. In this article, the coverage and downlink performance of HAP wireless networks exploiting the TVWS spectrum is evaluated based on the carrier-to-interference ratio (CIR) and carrier-to-interference plus noise ratio (CINR) power distribution from multi-beam payload antenna. Moreover, the effect of side lobe level on the system performance is examined.

The rest of the paper is organized as follows: Section 2 provides TVWS broadband services from the HAPs; Section 3 presents the co-channel interference system model; Section 4 presents the analysis and discussions of the simulation results; Finally, Section 5 presents the concluding remarks summarizing the key findings of the study.

2. TVWS Broadband Services from HAPs

Figure 1 below describes a HAP communications system configuration exploiting TVWS spectrums. The TVWS base stations are collocated on the platform employing a multi-beam antenna operating on UHF bands for the service link. In this scenario, a 121-cell system has been considered employing a cluster size of 4 cells. For HAP communications via TVWS spectrums, it's very important to consider the movements HAP may experience during its flight and as a result the movement of the individual cells. Such movements can greatly impact communication links, for example, by degrading communication quality and causing excessive signaling due to numerous handovers. As of [7][8], beam forming techniques and antenna configurations, which fix the location of cells have been investigated as a solution to prevent such issues regardless of the movement of HAP.

The authors attempted to demonstrate that digital beam forming will regulate beam direction to offset the movement of HAP, implying that cell location is unaffected by HAP position. In this work, we assume that regardless of HAP movement, cell positions remain static.

As per the authors in [15]-[17], the availability of TVWS is high in African countries like Ethiopia. The authors tried to investigate the amount of TVWS free spectrums by using a geolocation white spectrum database (GLSD) while employing the CSIR Calculation Engine (CSIR-CE) [16][17]. Based on this, we have considered

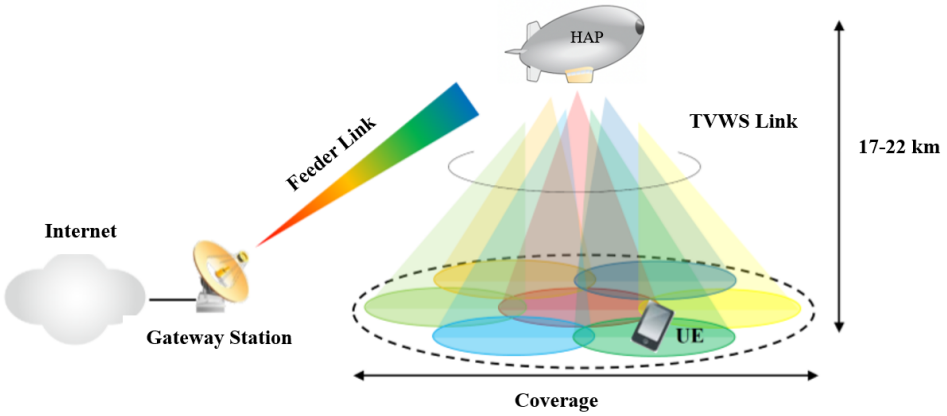

Fig. 1. HAP system configuration via TVWS spectrums [9]

employing the TVWS spectrums on HAPs so as to deliver wide area and affordable capacity wireless broadband for suburban and rural areas. For this work, we consider using off-the-shelf TVWS communication technology on board the HAP, such as the IEEE 802.22. This is the first TVWS standard envisaged

[19] for offering wireless access for rural area coverage of up to 100km. Installing IEEE 802.22 base stations on HAPS can provide even larger areas of wireless broadband service, by employing multi-beam antennas thus creating a TVWS cellular network. In this paper, we evaluate the coverage and performance of TVWS broadband from HAPs and illustrate the effectiveness of the system. The scenario illustrated in Figure 5 is considered. The scenario consists of a single HAP at 17 km altitude with a multi-beam antenna payload for serving multiple cells. The HAP system coverage area and cell radius are assumed to be 100 km and 10.5 km, respectively. Furthermore, hexagonally arranged cells which are clustered in 4 frequency-reuse patterns for covering the service area are assumed as depicted in Figure 4.

2.1. *Coverage Model for HAP Wireless Networks Exploiting TVWS Spectrum*

HAP TVWS coverage area can be determined by using the minimum elevation angle and the line-of-sight path loss model, radius of the earth, and height of the system as can be seen in Figure 2.

The surface area coverage can be determined using

$$S = \int_0^{2\pi} d\phi \int_0^{\varepsilon} d\varepsilon \left(R^2 sin\varepsilon\right) = 2\pi R^2 \left(1 - cos\varepsilon\right) \tag{1}$$

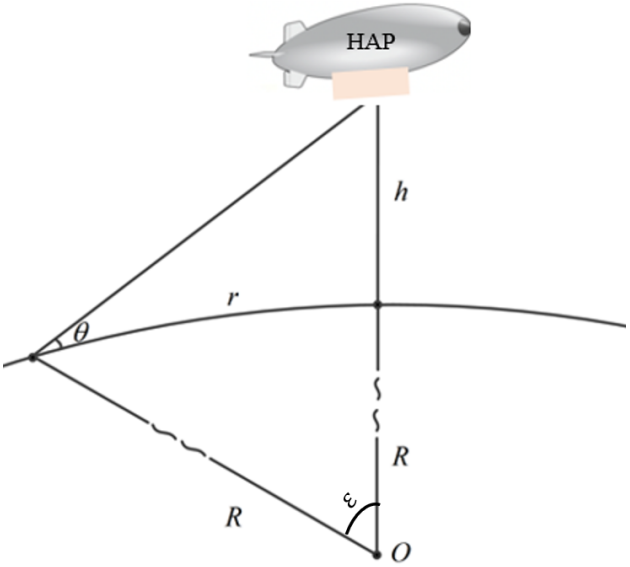

Fig. 2. Coverage model of HAP

Where

$$cos\varepsilon = \frac{cos^2\theta}{\frac{H}{R}+1} + sin\theta\sqrt{1-\frac{cos^2\theta}{\left(\frac{H}{R}+1\right)^2}} \tag{2}$$

Furthermore, the distance and elevation angle can be related as (3)

$$d = \frac{cos\varepsilon\,(R+H)-R}{Sin\theta} \tag{3}$$

Where R is the radius of the earth, h is the altitude of HAP and θ is minimum elevation.

2.2. *Cellular Configuration in the HAP TVWS system*

Cellular system interference is usually caused by users or cells operating on the same frequency causing co-channel interference or operating on adjacent frequencies causing adjacent channel interference. Interference can sometimes be caused by non-cellular systems. The solution to prevent co-channel interference is separating co-channel cells by a certain distance to get sufficient isolation between co-channel cells. The ratio of cell radius (R) and re-use distance (D) is the co-channel interference ratio (D/R *or* Q). D is the distance between the center of the cell interest and the centers of the nearest co-channel cells. Co-channel cell separation distance can be increased whenever D/R is increased. Thus, the interference is minimized. According to [20], for a hexagonal cell geometry the co-channel interference reduction factor, Q is given by:

$$Q = D/R = \sqrt{3N} \tag{4}$$

where N is a cell reuse factor. Lowering the value of Q provides more capacity or improved spectral efficiency, as doing so lowers the value of N. In this article, HAP based on the TVWS spectrums, hexagonally arranged cells grouped in a variety of frequency reuse patterns were examined. N is the number of frequencies to be reused in the cellular system in this scenario, and $1/N$ is the frequency reuse ratio. N may be derived by assuming hexagonal geometry [20]:

$$N = I^2 + I.J + J^2 \tag{5}$$

where $I.J = 0, 1, 2, 3, ..$etc). The following approaches should be used to locate the closest co-channel cell. (1) move i cells along any chain of hexagons, and (2) turn 60 anti-clockwise and move j cells as can be seen in Figure 3 below for i $= 3$ and j $= 2$ as discussed in [20].

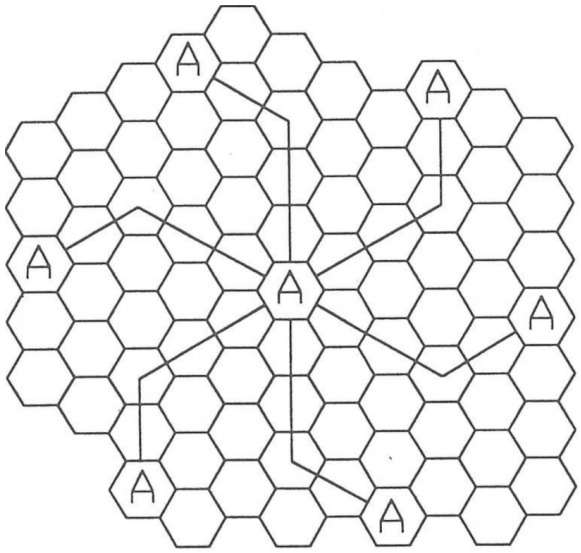

Fig. 3. How to locate the co-channel cells [20]

Locating a particular co-channel cell in a given cluster can be identified using

$$D = \sqrt{(i^2 + ij + j^2)}\left(R\sqrt{3}\right) \tag{6}$$

where R is the cell radius at the center of the hexagons. Figure 4 represents hexagonal cell arrangements for a 4 reuse pattern.

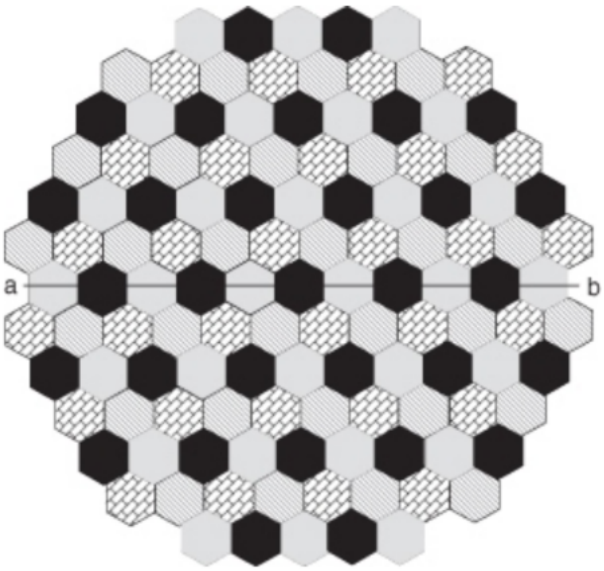

Fig. 4. Hexagonal cells for a 4-reuse pattern

2.3. *Multi-beam HAP Antenna Pattern*

The proposed HAP communication architecture exploiting the TVWS spectrum considers cells formed by beams generated from multi-beam antennas onboard the platform, just like in satellite communication systems. System performance is highly dependent on the gain of the antenna being optimized in the desired direction. This means proper antenna adjustment is essential. In an optimal cellular environment, an antenna pattern will radiate consistent power through its serving cell, with no power falling beyond the cell. However, in practice, power falling outside the coverage area occurs which results in interference to other neighboring cells. Therefore, in this work, a directional antenna pattern is considered, in order to provide more power radiation in the desired directions, thus preventing power from dropping in unwanted directions on the HAP and ground user [21][26]-[33]. Antenna pattern affects system QoS and network performance by determining the footprint, coverage area, interference, and CIR values. Each antenna in the HAP payload is directed to a different place within the coverage region. For each cell, the gain is subject to angles from the boresight (i.e. θ and φ) [21]:

$$A_{HAP}(\varphi) = \frac{32ln2}{2\left(2arccos\left(\sqrt[nH]{\frac{1}{2}}\right)\right)^2}\left(max\left(cos(\theta)^{nH}\right), S_f\right) \tag{7}$$

$$A_{User}(\theta) = G_{User\_boresight}\left(max\left(cos(\theta)^{nU}\right), S_f\right) \tag{8}$$

where nH is the roll-off rate for the HAP antennas, nU is the roll-off rate for user antennas. To prevent interference from other nearby systems on the same frequency, the user antenna be extremely directional.

2.4. *System Path Loss*

Due to the fact that HAPs offer LoS communication, the Free Space Path Loss (FSPL) model is extensively utilized for analyzing HAP systems. According to [21], FSPL can be determined as

$$FSPL_{HAP} = \left(\frac{4\pi d}{\lambda}\right)^2 \tag{9}$$

Where d is defined as the link distance, and λ is the wavelength of the signal. To represent the FSPL in dB, we may use the following:

$$FSPL_{HAP}\,(dB) = 92.4 + 20log\,(f_{GHz}) \; + 20log\,(d_{km}) \tag{10}$$

considering the link distance d in kilometers and frequency in gigahertz.

3. Co-Channel Interference System Model

In this article, a single HAP flying at a height of 17 kilometers with multibeam antennas serves as a base station for establishing a cell footprint on the ground. HAP, which is equipped with a multi-spot-beam phased array antenna, would be responsible for generating the ground cells. We split the HAP service zone into 121 cells in this study to create a suitable model of a prospective cell capable of creating co-channel interference. As can be seen in the co-channel interference model of Figure 5, Cell 1 is assumed to be the cell where our user-of-interest is located (reference cell). When it tries to communicate with the other HAP antenna such as cell 120, the user interferes with the HAP antennas 120 and 121, when they are operating the same frequency band as that of cell 1, since the individual HAP antenna has its boresight footprint in the center of the corresponding cell. As seen in Figure 5, the platform payload has a large number of base stations. The user test is done in the center of a reference cell that has been compromised by co-channel interference caused by another user. As a consequence, two factors are added to the user's location, namely the azimuth angle, φ_{H}, and the user's distance from the cell center (d). Using φ_{H} and d, CIR) and CINR of each user location can be determined, which in turn affects the system performance. Therefore, performances of the proposed scenario that is HAP-TVWS system downlink will be evaluated considering the coverage, CIR, CINR, and sidelobe labels as described in detail in the following equations.

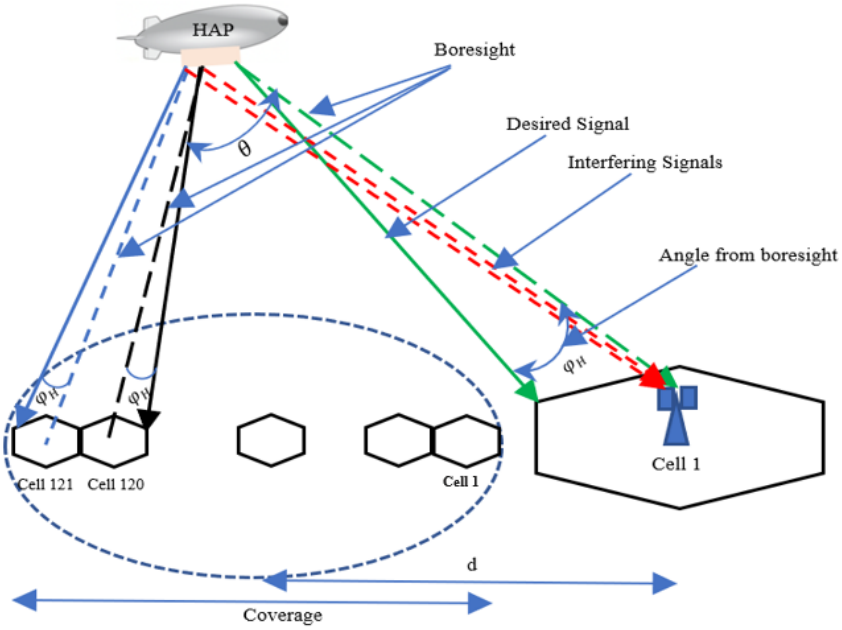

Fig. 5. Interference geometry from HAP communication system exploiting TVWS spectrums: Co-channel interference scenario

Calculations of the elevation and azimuth angles subtended by the circle of radius r that encloses the cell using the cell geometry shown in Figure 5 [2][22]-[24]

$$\theta_{sub} = tan^{-1}(g + r/h) - tan^{-1}(g - r/h) \tag{11}$$

$$\emptyset_{sub} = 2tan^{-1}\left(r/\sqrt{g^2 + h^2}\right) \tag{12}$$

The ground distance from the sub-platform point (SPP) to the cell center, as illustrated in 6, is denoted by g. In addition, the HAP's height is denoted by h.

Using Fig.7 as a guide, we can calculate the elevation $(\theta_0))$ and azimuth $(\emptyset_0)$ pointing angles from the HAP to the middle of each cell as follows:

$$\theta_0 = tan^{-1}\left(\frac{g}{h}\right) \tag{13}$$

$$\emptyset_0 = sin^{-1}\frac{(c-1)\,dsin\frac{\pi}{3}}{g} + (n_s - 1)\frac{\pi}{3} \tag{14}$$

As seen in Figure 7, the multibeam antenna on HAPS will have a number of cells on the field, with each cell being represented by $(\mathrm{n_r}, \mathrm{n_c})$ which are the number

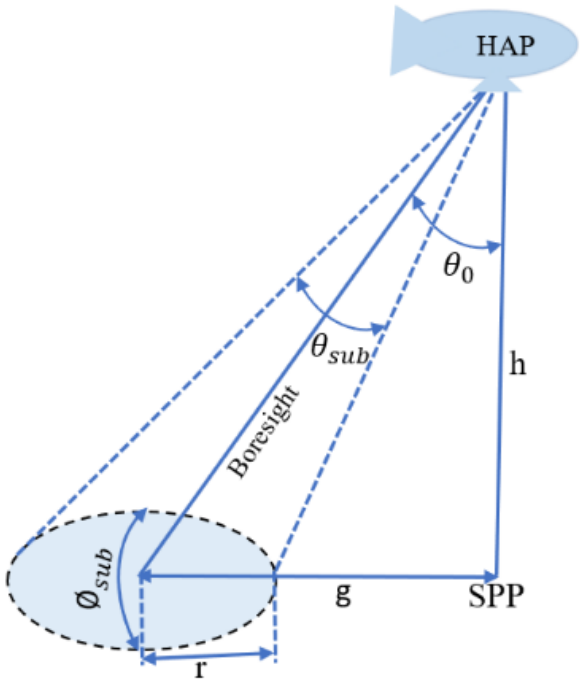

Fig. 6. Cell geometry from HAP communication system exploiting TVWS spectrums

of the concentric hexagonal ring n_r and the number of the cell inside the ring n_c, $1 \leq n_c \leq 6n_r, n_r \neq 0$

The cosine law may be used to calculate g as follows

$$g = \sqrt{(n_r d)^2 - (c-1)\, d^2 - 2n_r d^2\, (c-1)\, cos\frac{\pi}{3} r} \tag{15}$$

Where d is the hexagon's width and c is the cell's position in relation to the first cell's side.

$$c' = n_c - (n_s - 1)\, n_r \tag{16}$$

where n_s is an integer number between 1 and 6 on each side of the hexagon

$$n_s = 1 + Floor\left[\frac{n_c - 1}{n_r}\right] \tag{17}$$

The $floor$ is an integer operator. The directivity (D_{max}) of antennas that have main lobe patterns determined by a cosine function raised to a power n [2].

$$D = D_{max}(cos\theta)^n \tag{18}$$

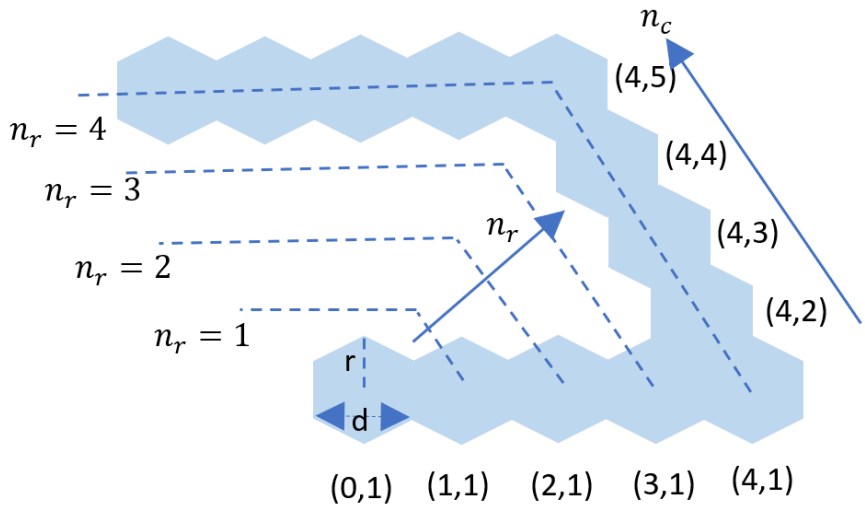

Fig. 7. Hexagonal cell structure coordinate scheme

where θ is the angle relative to the antenna boresight, and n is the factor roll-off. At every location (x, y) on the ground, there is a directivity that may be found.

Where

$$D_{max} = \frac{32ln2}{\left(2arccos\left(\sqrt[n_\theta]{\frac{1}{2}}\right)\right)^2 + \left(2arccos\left(\sqrt[n_\theta]{\frac{1}{2}}\right)\right)^2} \tag{19}$$

Where $n_\emptyset$ and n_θ are roll-off rates of the azimuth and elevation respectively. Considering the ground receivers are always connected to the strongest cell, the received power is equal to

$$P_{max}(x, y) = max\left[P_T G_U D\left(\frac{\lambda}{4\pi d}\right)^2\right] =$$

$$P_T G_U \left(\frac{\lambda}{4\pi d}\right)^2 [D]max \tag{20}$$

where P_T denotes HAPs' transmitter power, D denotes directivity gain and G_U denotes receiver antenna gain.

CIR [2] for the co-channel cells category may be computed once the power in a point (x, y) is determined (21).

$$CIR(x, y) = \frac{P_{max}(x, y)}{\sum_{i=1}^{121} P_i(x, y) - P_{max}(x, y)} \tag{21}$$

The footprint size and coverage area heavily depended on the required ground CIR value. The bandwidth efficiency can be obtained from the CIR which has been determined across the coverage area using

$$\eta \approx log_2\left(1 + CIR\right) \tag{22}$$

The CINR can be obtained using

$$CINR = \frac{log_2 MR_b}{B_n + I/N_0} SNR \tag{23}$$

Where

$$I = \sum_{m=1}^{N_H} \frac{P_{HAP-TVWS_m} G_{HAP-TVWS}\left(\varphi\right)_m G_{User}\left(\theta\right)_m}{L_{feeder_m} P_{FSPL_m} A_{atm_m}} \tag{24}$$

Where the index denotes the interfering HAP interfering beams that cause co-channel interference, (i.e. $m = 1, 2, \ldots..121$). I is the aggregate interference power from m multibeam HAP antennas, Bn denotes the noise bandwidth of the receiver, Rb, M and N_0 denotes the bit rate, M-ary, and noise power spectral density respectively. $P_{HAP-TVWS}$ is the transmit power of the HAP base station exploiting TVWS spectrums. $G_{HAP-TVWS}\left(\varphi\right)$ is the HAP base station transmitting antenna gains in directions φ degrees off the beam center, $G_{User}\left(\theta\right)$ is the receiving antenna gain of the ground consumer in the direction of the m^{th} HAP base station and L_{feeder} is the ground user receiving antenna feeder loss, L_{FSPL} is the free space loss and A_{atm} represent the atmospheric absorption. Finally, the sidelobe level system performance is a critical problem that will impact inter-cell interference and system capacity.

3.1. *Sidelobe Levels*

In spite of the fact that frequency reuse schemes are employed to reduce the co-channel interference, in HAPS cellular system communications, a high level of sidelobes of the on-board antenna might be prone to unwanted effects. Whenever spot beams are needed to provide a cluster of footprints, the power of individual beams must be bounded in the cell boundary. Beams with significant side lobe levels might cause interference with neighboring cells. The effect of the interferences can be assessed by determining the signal-to-noise ratio (SNR) between the power of the desired signal ($P_{max}(x, y)$) and the noise power (P_N) at each point of the ground. In this case, the noise power is the sum of the thermal noise ($\mathrm{N_T}$) and the power ($P_i\left(x, y\right)$) of all the neighbor beams i which are using the same frequency of the desired signal. Thus,

$$SNR = \frac{P_{max}(x, y)}{P_N} = \frac{P_{max}(x, y)}{N_T + \sum_{i=1}^{N_f} P_i\left(x, y\right)} \tag{25}$$

where N_f is the number of neighbors that use the same frequency with the desired signal. The cells using the same frequency are far sufficient to consider the power of an interfering signal and can be obtained by:

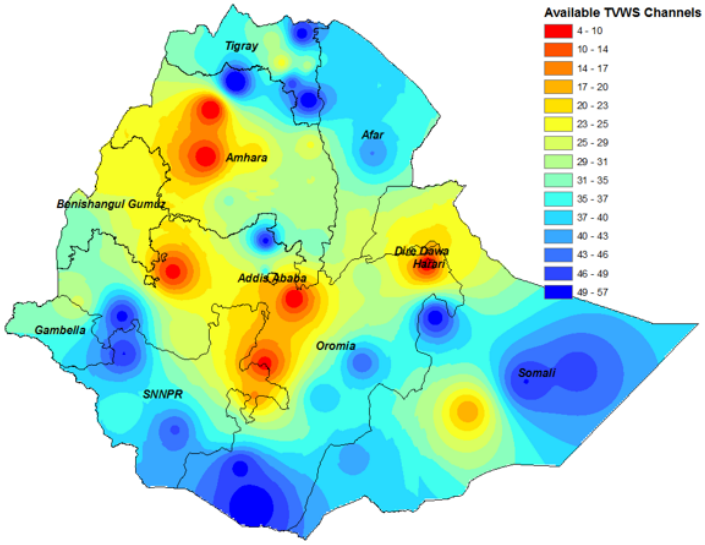

Fig. 8. Heat map depicting maximum available TVWS channels for the entire Ethiopia

$$P_i\left(x,y\right) = P_{max}(x,y)s_{LL} \tag{26}$$

Yielding,

$$CNR = \frac{P_{max}(x,y)}{P_N} \approx \frac{P_{max}(x,y)}{N_f P_i\left(x,y\right)} \approx \frac{1}{N_f s_{LL}} \tag{27}$$

Where s_{LL} side lobe label. As can be seen from equation (27), s_{LL} of the onboard antenna is crucial in demonstrating the system's performance.

4. Simulations Results and Discussion

Figure 8 illustrates the map of Ethiopia indicating the available TVWS channels in the VHF and UHF TV bands across the country. The heatmaps graphically illustrate that many parts of Ethiopia can benefit from the TVWS spectrum availability especially the ones in the rural areas that can support different services / different speeds whenever and wherever possible. Taking advantage of this opportunity, we have considered installing TVWS base stations on HAP using the available free spectrums so as to provide a large coverage and affordable connectivity for suburban and rural areas

For improving the spectral efficiency and signal quality, frequency reuse is one of the solutions. As can be seen from Figure 9, when the cluster size in a given cellular tessellation is increased the frequency reuse distance is also increased. A large value of D/R provides lower interference since the cluster size N is large even though there is a tradeoff with capacity. Figure 10 shows the HAP coverage area

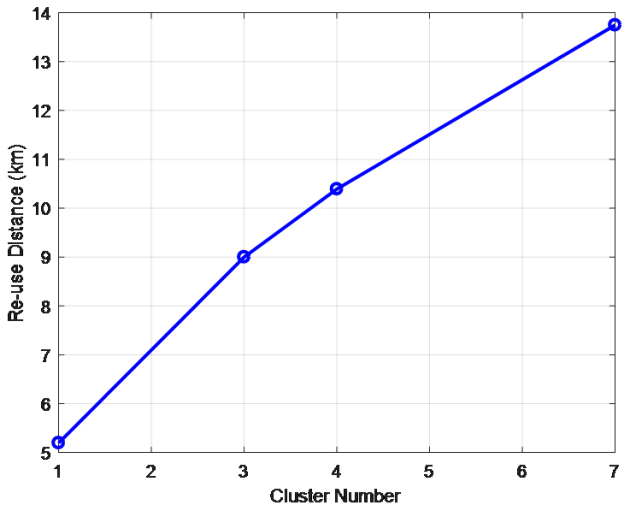

Fig. 9. Relationship between cluster number and reuse distance

using the TVWS link. Communication coverage from a single HAP can replace the number of cellular communication system base stations. The coverage area can be increased as the elevation angle gets smaller. Figure 11 illustrates the relationship between propagation loss and distance between HAP to a user. As the distance between HAP to a user increases, the loss increases as well.

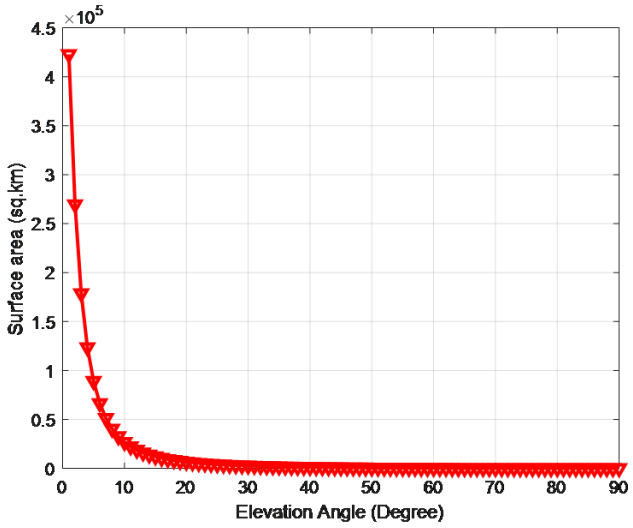

Fig. 10. Surface area coverage of HAP-TVWS

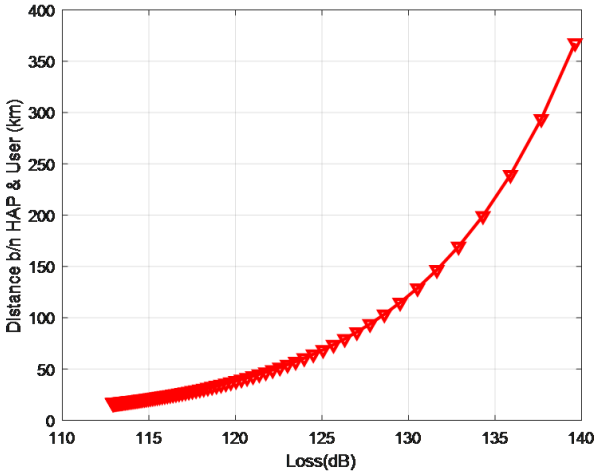

Fig. 11. Loss as a function of distance between HAP and user

HAP cellular system performance exploiting TVWS spectrums was evaluated in terms of CIR and CINR for downlink communications. The CIR performance and cumulative distribution function (CDF) as well as CINR contour are investigated as can be seen in Figure 12 and 13 respectively.

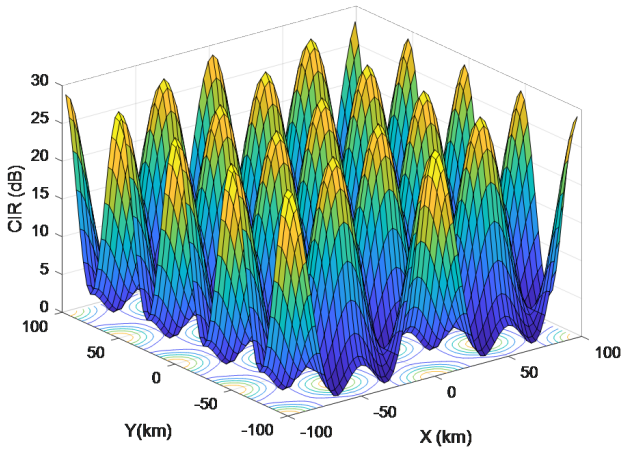

Fig. 12. CIR contour of maximum power distribution for aperture antenna model

As seen in Figure 12, users positioned in the cell's center experience the highest

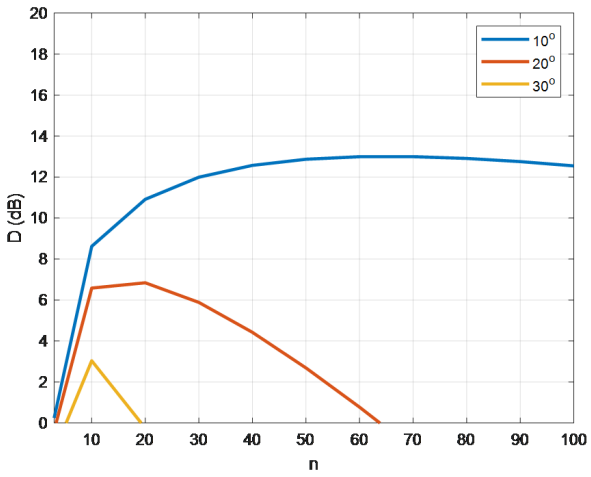

Fig. 13. Directivity versus n at edge of cell

CIR. When they approach the cell edge, CIR decreases by a five dB range.

Figure 13 indicates that for a given number of n, the directivity is maximum at a certain angle subtended at the cell edge. As seen in the diagram, the value of n would be 10, 20, and 30. The narrower beamwidth increased antenna directivity but decreased elevation angle range. Figure 13 illustrates the influence of power roll-off on directivity. From Figure 13, it can be seen that to maximize the power at the edge of a cell subtending 10, 20, and 30 at the HAP, the value of $n = 60$ is chosen. As can be seen from Figure 13, the directivity is maximum at the minimum subtended angle and maximum roll-off factor and it is minimum at a higher minimum subtended and minimum power roll-off factor.

If the beamwidth is too small, excessive power rolls off at the cell's edge is created and if the beamwidth is too broad, excessive power falls outside the cell.

Figure 14 shows the user antenna radiation mask. Three separate side lobe floor values of -30dB, -25dB, and -20dB are seen in the diagram. To avoid interference from other devices using the same frequency, the user antenna should be highly directional.

The HAP antenna radiation masks for 5, 8, and 12 values of nH are shown in Figure 15. The figure clearly shows how the antenna directivity increases as the roll-off factor increases. As a result, as the roll-off factor increases, the antenna beam width reduces.

Figure 16 depicts the cumulative distribution function (CDF) of the downlink CINR of HAP using the TVWS spectrum. On average, TVWS downlink services may be delivered at a level of around 28 dB. As can be seen from Figure 17, the sidelobe level plays an important role in demonstrating the system's performance. The figure shows maximum SNR is achieved at $-40dB$ and SNR is used to compute

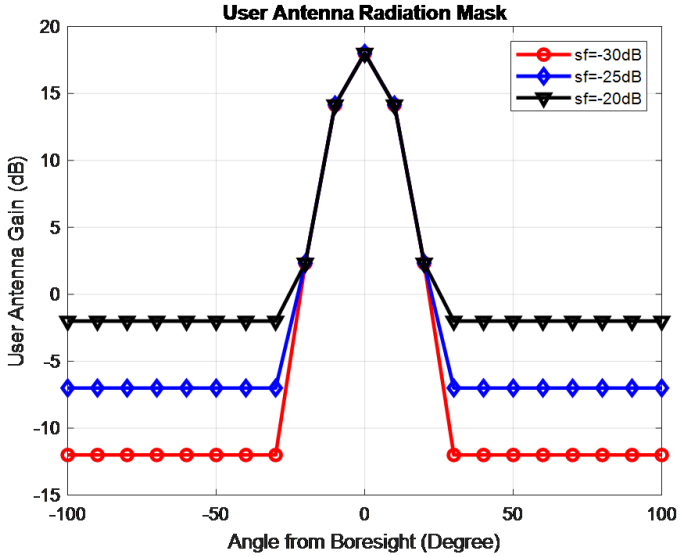

Fig. 14. FUser antenna radiation mask at different sidelobe floor

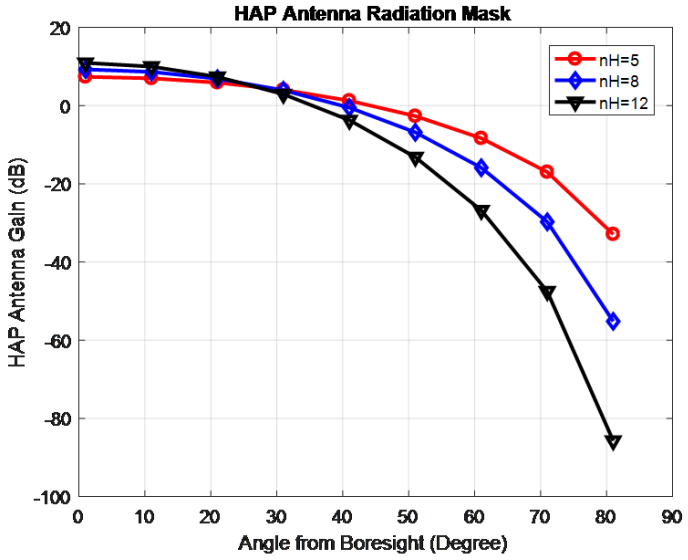

Fig. 15. HAP antenna radiation mask at different values of nH

CINR.

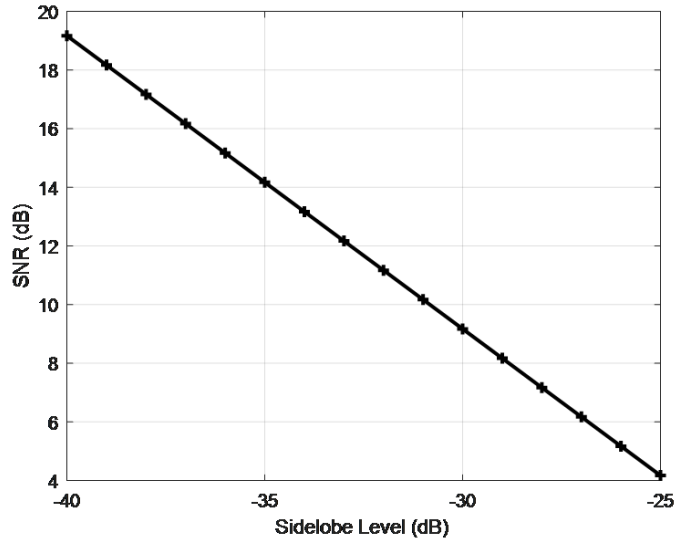

Fig. 17. Relationship between sidelobe level and SNR

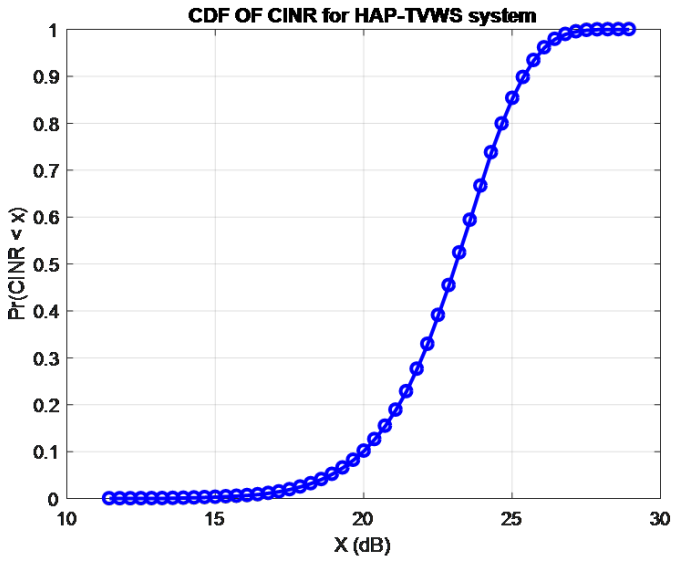

Fig. 16. CDF of CINR of HAP TVWS system

5. Conclusions And Future Works

5.1. *Conclusions*

In this paper, we proposed using a multibeam antenna payload to deploy a HAP system exploiting TVWS spectrums. The feasibility of the suggested scenario co-channel interference is then assessed using computer simulation in terms of CIR and CINR. Co-channel interference caused by HAP using the TVWS communications network is dependent on the antenna beam width, angular separation, and sidelobe level. The HAP antenna radiation masks for 5, 8, and 12 values of nH are compared. How the antenna directivity increases as the roll-off factor increases is investigated. The effect of the sidelobe level is demonstrated so as to show its impact on system performance.

5.2. *Future Works*

The logical next step in expanding this article is taking user mobility into account. It is fascinating to see how the system responds to mobile users and how to best serve them. This would include determining whether beam tracking and steering or frequent handovers are more suited to serving mobile users. Artificial intelligence and machine learning may play a key role in beam steering and handover by offering mobility prediction. Additionally, more research may be done to determine how the HAP's location in relation to the service area's center affects the system's capacity and coverage. Moreover, the work that is presented in this article is based on the assumption that the HAP is, for the most part, stationary. On the other hand, it might be worthwhile to research dynamically altering the HAP's location to shorten either individual or total connection lengths.

References

1. Karapantazis S. and Pavlidou F. (2005). Broadband communications via high-altitude platforms: A survey. IEEE Communications Surveys & Tutorials, vol. 7, no. 1, pp. 2-31.
2. Thornton J., Grace D., Capstick M. H., and Tozer T. C. (2003). Optimizing an array of antennas for cellular coverage from a high-altitude platform. IEEE Transactions on Wireless Communications, vol. 2, no. 3, pp. 484492, May 2003.
3. Alsamhi S. H. and Rajput N. S.(2014). HAP antenna radiation pattern for providing coverage and service characteristics. International Conference on Advances in Computing, Communications and Informatics (ICACCI), New Delhi, pp. 1434-1439.
4. Iskandar, Gratsia S., and Ernawan M. E. (2017). LTE uplink cellular capacity analysis in High-Altitude Platforms (HAPS) communication. 11th International Conference on Telecommunication Systems Services and Applications (TSSA), Lombok, pp. 1-5.
5. Yang Z., Mohammed A., and Hult T. (2007). Uplink Performance Evaluation

of WiMAX Broadband Services via High Altitude Platforms (HAPs). The Second European Conference on Antennas and Propagation, EuCAP 2007, Edinburgh, pp. 1-5.

6. Siahaan K. G. and Iskandar. (2016). Performance improvement on the Downlink HAPS communication channel employing MIMO antenna. 10th International Conference on Telecommunication Systems Services and Applications (TSSA), Denpasar, pp. 1-4.
7. Hoshino K. et al. (2018). A Study on Service Link Antenna Considering Fixed Footprint in HAPS System," IEICE Technical Report, vol. 118, no. 310, AP2018-118, pp. 95-100.
8. Sudo S., et al. (2018). A Study on Beam Pattern in Horizontal Plane in HAPS SystemIEICE Technical Report, vol. 118, no. 310, AP2018-119, pp. 101-106.
9. Shibata Y., Kanazawa N., Hoshino K., Ohta Y., Nagate A. (2019). A Study on Cell Configuration for HAPS Mobile Communications. IEEE 89th Vehicular Technology Conference (VTC2019-Spring), Kuala Lumpur, Malaysia, pp. 1-6, doi: 10.1109/VTCSpring.2019.8746491.
10. Thornton J., Grace D., Spillard C., Konefal T., and TozerT. (2001). Broadband communications from a high-altitude platform: The European HeliNet program. Electronics & Commun. Engineering J., vol. 13, no. 3, pp. 138-144.
11. Karapantazis S., and Pavlidou F. (2005). The role of high altitude platforms in beyond 3G networks," IEEE Wirel. Commun., vol. 12, no. 6, pp. 33-41.
12. Biswas P.K. (2010). A formal framework for multicast communication. EEE Syst. J., vol. 4, no. 3, pp. 353-362.
13. Dong F., Li H., Gong X., Liu Q., and Wang J. (2015). Energy-efficient transmissions for remote wireless sensor networks: An integrated HAP/satellite architecture for emergency scenarios. Sensors, vol. 15, no. 9, pp. 22266-22290.
14. Mishra A.K., and Johnson D.L. (2015). White Space Communication: Advances, Developments and Engineering Challenges (Signal and Communication Technology). Springer Publication.
15. OFCOM. (2012). Regulatory Requirements for White Space Devices in the UHF TV Band.
16. Hussien H.M., Katzis K., Mfupe L.P., and Bekele E.T. (2019). Coexistence of TV White Space Devices and DTV Services in Ethiopian Geolocation White Space Spectrum Database. IEEE 24th International Workshop on Computer-Aided Modeling and Design of Communication Links and Networks (CAMAD), pp. 1–5.
17. Hussien H.M., Katzis K., Mfupe L.P., and Bekele E.T. (2019).Practical Implementation of Geo-location TVWS Database for Ethiopia. ICAST 7th EAI International Conference on Advancements of Science and Technology, p. 6.
18. IEEE 802.22. (2019). Working Group on Wireless Regional Area Networks. Functional Requirements for the 802.22 WRAN. Doc#: IEEE 802.22-05/0007r46.

19. Stevenson C.et al. (2009). IEEE 802.22: The First Cognitive Radio Wireless Regional Area Network Standard. IEEE Communications Magazine, vol.47, no. 1, pp. 130-138.
20. Rappaport T. (2001). Wireless Communications: Principles and Practice, second ed. Prentice Hall PTR, Upper Saddle River, NJ, USA.
21. Katzis K., Mfupe L., and Mohammed H. (2020). Opportunities and Challenges of Bridging the Digital Divide using 5G enabled High Altitude Platforms and TVWS Spectrum. IEEE Eighth International Conference on Communications and Networking (ComNet).
22. El-Jabu B. and Steele R. (2001). Cellular communications using aerial platforms. IEEE Trans. Veh. Technol., vol. 50, pp. 686—700.
23. Iskandar, Abubaker A. (2014). Co-channel Interference Mitigation Technique for Mobile WiMAX Downlink System Deployed via Stratospheric Platform.8^{th} International Conference On Telecommunications Systems Services And Applications.
24. Thornton J. (2004). Properties of spherical lens antennas for high altitude platform communications. 6th European Workshop on Mobile/Personal Satcoms and 2nd Advanced Satellite Mobile Systems (EMPS & ASMS), ESTEC, European Space Agency.
25. He P., Cheng N., and Cui J. (2016). Handover performance analysis of cellular communication system from high altitude platform in the swing state. IEEE International Conference on Signal and Image Processing (ICSIP).
26. Hussien H.M., Katzis K., Mfupe L.P., and Bekele E.T. (2022). Capacity, Coverage and Power Profile Performance Evaluation of a Novel Rural Broadband Services Exploiting TVWS From High Altitude Platform. IEEE Open Journal of the Computer Society, vol. 3, pp. 86-95., doi: 10.1109/OJCS.2022.3183158.
27. Hussien H.M., Katzis K., Mfupe L.P., and Bekele E.T. (2022). Performance Optimization of High-Altitude Platform Wireless Communication Network Exploiting TVWS Spectrums Based on Modified PSO. IEEE Open Journal of Vehicular Technology, vol. 3, pp. 356-366, doi: 10.1109/OJVT.2022.3191762.
28. Hussien H.M., Katzis K., Mfupe L.P., and Bekele E.T. (2022). Bridging the Urban-Rural Broadband Connectivity Gap using 5G Enabled HAPs Communication Exploiting TVWS Spectrum. Journal of Engineering Research and Sciences, Volume 1, Issue 2, Page # 24-32; ISSN: 2831-4085.
29. Hussien H.M., Katzis K., Mfupe L.P., and Bekele E.T. (2021). Calculation of TVWS Spectrum Availability Using Geo-location White Space Spectrum Database. IEEE AFRICON, pp. 1-6, doi: 10.1109/AFRICON51333.2021.9570915.
30. Hussien H.M., Meko S.F., Katzis K., L. P. Mfupe L.P., and Bekele E.T. (2022). Bridging the Urban-Rural Broadband Connectivity Gap using 5G Enabled HAPs Communication Exploiting TVWS Spectrum. Journal of Engineering Research and Sciences, Volume 1, Issue 3, Page # 98-105;

DOI:10.55708/js0103010

31. Hussien H.M., Katzis K., and Mfupe L.P. (2021). Dynamic Spectrum Allocation for TVWS Wireless Access from High Altitude Platform. International Conference on Electrical, Computer and Energy Technologies (ICECET), pp. 1-6, doi: 10.1109/ICECET52533.2021.9698667.
32. Hussien H.M., Katzis K., and Mfupe L.P. (2021). Intelligent Power Allocation for Cognitive HAP Wireless Networks Using TVWS Spectrum. International Conference on Electrical, Computer and Energy Technologies (ICECET), pp. 1-6, doi: 10.1109/ICECET52533.2021.9698778.
33. Hussien H.M., Meko S.F., Katzis K., L. P. Mfupe L.P., and Bekele E.T. (2021). A Novel Resource Allocation for HAP Wireless Networks Exploiting TVWS Spectrum. IEEE AFRICON, pp. 1-6, doi: 10.1109/AFRICON51333.2021.9570928.